Growth of CuCl thin films by magnetron sputtering for ultraviolet optoelectronic applications

Gomathi Natarajan[a] and S. Daniels
Nanomaterials Processing Laboratory (NPL), NCPST, Dublin City University, Dublin-9, Ireland

D. C. Cameron
Advanced Surface Technology Research Laboratory (ASTRaL), Lappeenranta University of Technology, 50101 Mikkeli, Finland

L. O'Reilly, A. Mitra, P. J. McNally, and O. F. Lucas
Nanomaterials Processing Laboratory (NPL), RINCE, Dublin City University, Dublin-9, Ireland

R. T. Rajendra Kumar and Ian Reid
School of Physical Sciences, Dublin City University, Dublin-9, Ireland

A. L. Bradley
Semiconductor Photonics Group, Physics Department, Trinity College, Dublin 2, Ireland

(Received 27 October 2005; accepted 9 June 2006; published online 9 August 2006)

Copper (I) chloride (CuCl) is a potential candidate for ultraviolet (UV) optoelectronics due to its close lattice match with Si (mismatch less than 0.4%) and a high UV excitonic emission at room temperature. CuCl thin films were deposited using radio frequency magnetron sputtering technique. The influence of target to substrate distance (d_{ts}) and sputtering pressure on the composition, microstructure, and UV emission properties of the films were analyzed. The films deposited with shorter target to substrate spacing (d_{ts}=3 cm) were found to be nonstoichiometric, and the film stoichiometry improves when the substrate is moved away from the target (d_{ts}=4.5 and 6 cm). A further increase in the spacing results in poor crystalline quality. The grain interface area increases when the sputtering pressure is increased from 1.1×10^{-3} to 1×10^{-2} mbar at d_{ts}=6 cm. Room temperature cathodoluminescence spectrum shows an intense and sharp UV exciton (Z_3) emission at ~385 nm with a full width at half maximum of 16 nm for the films deposited at the optimum d_{ts} of 6 cm and a pressure of 1.1×10^{-3} mbar. A broad deep level emission in the green region (~515 nm) is also observed. The relative intensity of the UV to green emission peaks decreased when the sputtering pressure was increased, consistent with an increase in grain boundary area. The variation in the stoichiometry and the crystallinity are attributed to the change in the intensity and energy of the flux of materials from the target due to the interaction with the background gas molecules. © *2006 American Institute of Physics*. [DOI: 10.1063/1.2227261]

I. INTRODUCTION

UV/blue optoelectronic materials such as GaN and ZnO are typically grown on insulating substrates such as sapphire or SiC.[1] The use of silicon substrates offers obvious advantages, such as compatibility with microfabrication techniques and good thermal conductivity which would be a low cost alternative for device fabrication. Epitaxial growth of GaN and ZnO layers on silicon substrates has been demonstrated by a few research groups.[2–4] However, a large lattice mismatch of more than 17% between the hexagonal GaN and ZnO and the cubic Si is still an issue in the device fabrication. A large lattice mismatch between these films and the silicon substrate results in the formation of high dislocation densities and ultimately reduces the emission lifetime and reliability of the device.[5,6] CuCl has a cubic zinc-blende structure with a lattice constant, a_{CuCl}=5.41 Å,[7] which is close (mismatch <0.4%) to that of Si (a_{Si}=5.43 Å, diamond cubic).[8] This close match in the crystal system and lattice parameters of CuCl and Si opens up the possibility of realizing Si based UV photonic devices using CuCl as UV emitting layer with low defect density.

Furthermore, CuCl has a direct band gap of 3.39 eV and an exciton binding energy of 190 meV.[9] The binding energy is very high compared with other blue optoelectronic materials such as GaN (25 meV)[10] and ZnO (60 meV).[11] The high exciton binding energy, the exciton emission in UV, and the close lattice matching with Si make CuCl a potential candidate for Si based UV/blue emitting devices. There are a few reports on the growth mechanisms of the epitaxial CuCl layers on a number of substrates[12–18] focusing the fundamental growth process and interfacial analysis. The present investigation steps forward to the growth and characterization of a CuCl films mainly for UV optoelectronic device fabrication.

The growth of a defect-free CuCl–Si system with high optical quality is important for optoelectronic applications. Defect states including nonstoichiometry and dislocations play an important role as nonradiative recombination centers which are mainly attributed to near surface regions and grain

[a]Electronic mails: gomathi.natarajan@mail.dcu.ie and gomathinatarajan@yahoo.com

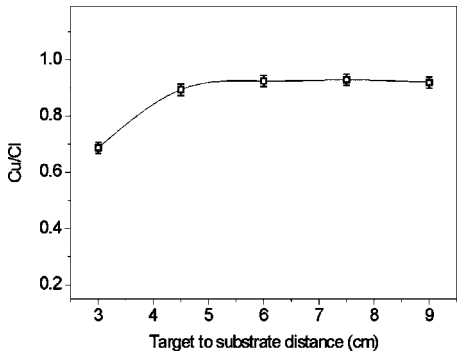

FIG. 1. Influence of target to substrate spacing on the composition (from EDX analysis). Note: The solid line is only a guide to the eyes.

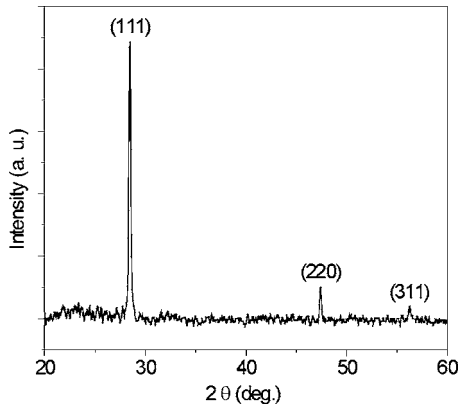

FIG. 2. XRD spectrum of CuCl film deposited at a target to substrate distance of 6 cm.

boundaries.[19–22] From the device point of view, the effects of chemical stoichiometry and microstructure on the optoelectronic properties are crucial. Optimizing the growth parameters is one of the key factors in obtaining high optical quality films. In this paper, we report on the growth of CuCl thin films by the rf magnetron sputtering technique and the influence of (i) target to substrate spacing and (ii) working pressure on the compositional, microstructural, and optoelectronic properties. The UV emission properties are analyzed using cathodoluminescence spectroscopy mainly considering the existence of meso- and nanostructural interfaces within the thin film.

II. EXPERIMENT

CuCl thin films were deposited using rf magnetron sputtering onto glass and Si(111) substrates, which were ultrasonically cleaned with acetone, trichloroethane, methanol, and de-ionized water. The CuCl target was presputtered for 10 min prior to deposition. Optical emission spectroscopy and electrical impedance monitoring of the magnetron source showed that this period of time was necessary to allow the sputtered flux to reach a steady state. The deposition chamber was pumped down to a base pressure of 1×10^{-7} mbar. The substrates were placed at various distances from the target, from 3 to 9 cm, at an argon gas pressure of 2×10^{-3} mbar. Film properties were also studied while varying the argon gas pressure from 1.1×10^{-3} to 1×10^{-2} mbar at a target to substrate spacing of 6 cm, which yielded stoichiometric CuCl films. The deposition was performed under constant conditions for 30 min, with the substrate unheated. Monitoring of the substrate temperature during deposition showed that it only increased by 6 °C. The power density at the target was 0.5 W/cm^2. The substrates were at floating potential. The thickness of the samples was 400 ± 20 nm.

The crystallinity of the CuCl films grown on glass substrates was examined by x-ray diffraction (XRD) analysis using a Bruker D8 AXS advance instrument with Cu $K\alpha$ radiation of wavelength of 1.54 Å. The XRD spectra were measured in the Bragg-Brentano (θ-2θ) geometry. Contact mode atomic force microscopy (AFM) analysis was performed using a Pacific Nanotechnology Nano-R AFM. Compositional analysis was performed by energy dispersive x-ray (EDX) analysis with a Leo Stereoscan 440 scanning electron microscope and a Princeton Gamma Tech energy dispersive x-ray analyzer with a Si(Li) detector. Film composition was analyzed relative to the target with an accelerating voltage of 14 kV and a probe current of 3 nA. Room temperature (RT) cathodoluminescence studies were performed using the LEO Stereoscan 440 scanning electron microscope with an electron beam of 4 keV and a probe current of 15 nA. The luminescence was collected by a parabolic mirror placed approximately 1 mm above the sample. The collected signal was then transferred to a Gatan MonoCL spectrometer equipped with a 1200 lines/mm grating. The spectral resolution was approximately 1 nm.

III. RESULTS

Figure 1 shows the variation in the Cu/Cl ratio of the film as a function of target to substrate spacing, obtained from EDX analysis for the films deposited at an Ar pressure of 2×10^{-3} mbar. The target to substrate spacing was found to have a strong influence on the properties of the films. A spacing of 3 cm from the target to substrate yields highly nonstoichiometric, i.e. chlorine rich, films. The film composition varies drastically when the target to substrate distance is increased from 3 to 4.5 cm. Nearly stoichiometric films were obtained for further increase in the spacing (6 cm). There was no noticeable variation in the stoichiometry for the spacing beyond 6 cm, and the films deposited at the positions 6, 7.5, and 9 cm from the target were found to have compositions close to that of the target (within the error limit). These experiments were performed several times to establish the veracity of the results.

X-ray diffraction spectra measured using the θ-2θ geometry for nearly stoichiometric CuCl film deposited at $d_{ts}=6$ cm is shown in Fig. 2. The most intense peak appears at $2\theta\sim28.45°$ corresponding to the (111) plane orientation. The other two less intense peaks centered at ~47.44° and 56.27° correspond to the (220) and (311) planes, respectively. It is well known that the crystalline quality is indicated by the width of the diffraction peak; a smaller width is an indication of better crystalline quality.[23] The full width at half maximum (FWHM) of the CuCl (111) peak was measured and the average crystallite size was estimated using the Scherrer formula.[23] Figure 3 shows the variation in FWHM and the corresponding average grain size (in right Y axis) as a func-

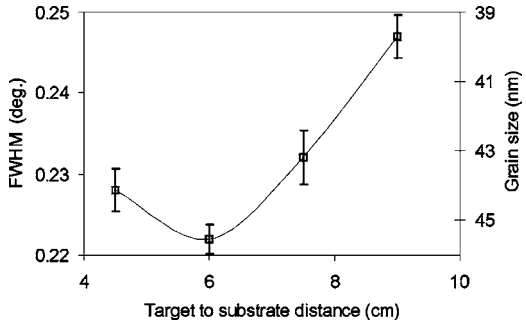

FIG. 3. Variation in FWHM of (111) peak with target to substrate spacing (grain size in the right *Y* axis).

tion of target to substrate distance for the near stoichiometric samples. The FWHM of (111) diffraction is minimum for $d_{ts}=6$ cm and then increases for other target-substrate separations, indicating a degradation in the crystalline quality. Thus, a target to substrate spacing of 6 cm was found to yield nearly stoichiometric CuCl thin films of better structural quality.

To investigate the influence of sputtering pressure on the film properties, a spacing of 6 cm was used and the background gas pressure was varied from 1.1×10^{-3} to 1×10^{-2} mbar. EDX analyses showed that all of the films were nearly stoichiometric, and a change in the working pressure had no major influence on the film stoichiometry. In addition no impurity elements were detected in the samples. The FWHM of the CuCl (111) plane diffraction peaks is measured and plotted as a function of the sputtering gas pressure, as shown in Fig. 4, and the corresponding average grain size is scaled in the right *Y* axis. The figure indicates that the FWHM increases (i.e., the grain size decreases) linearly with the increase in sputtering pressure. The average crystallite sizes were found to be approximately 40 and 30 nm for the samples deposited at 1.1×10^{-3} and 1×10^{-2} mbar, respectively.

AFM topographs of the samples deposited at 1.1×10^{-3} and 1×10^{-2} mbar are shown in Fig. 5. The images show that the samples consist of particles with mean sizes of around 450 and 280 nm for those deposited at 1.1×10^{-3} and 1×10^{-2} mbar, respectively. It is interesting to note that the grain size seen in atomic force microscopy (AFM) is much greater than that deduced from XRD analysis. Therefore, the

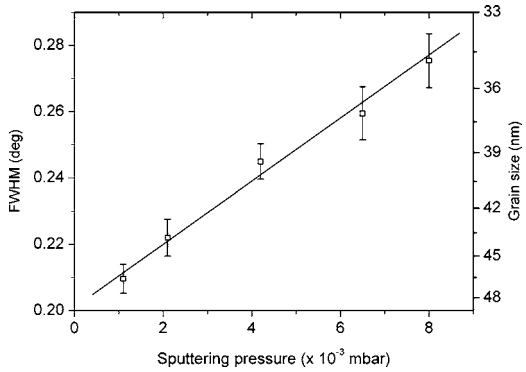

FIG. 4. Variation in the FWHM of the (111) XRD peak of CuCl thin films with sputtering pressure (grain size in the right *Y* axis).

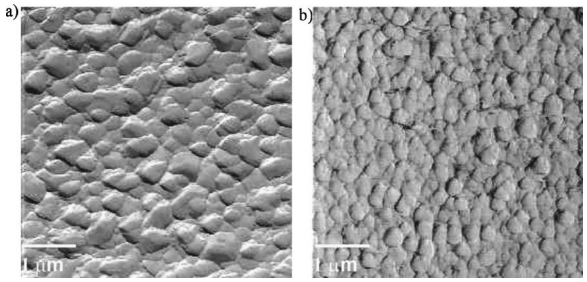

FIG. 5. AFM topographs of CuCl films grown at different sputtering pressures of (a) 1.1×10^{-3} mbar and (b) 1×10^{-2} mbar (scale bar = 1 μm).

grains observed in AFM topography can be considered as polycrystalline domains consisting of clusters of nanocrystallites. Moreover, two types of interfaces, viz., particle-particle and grain-grain are expected as shown in Fig. 6. The surface to volume ratio (S/V) of the grains increases as the particle size decreases, accompanied by a concomitant increase in grain boundary area. Hence, when the sputtering pressure is increased, the overall interface area (particle and grain) in the sample increases.

Figure 7 shows the room temperature CL spectra of the samples deposited with $d_{ts}=6$ cm at various indicated sputtering pressures. A very strong UV emission appears at $\lambda\sim385$ nm, which is due to the recombination governed by Z_3 excitons. A low intensity broad green emission centered at ~515 nm is also observed. Sub-band gap emission such as this is generally considered to originate from impurities, defects, and nonstoichiometry. Similar deep level emission is reported by several authors[24–26] for UV emitting ZnO thin films. There is a small increase in the FWHM of the Z_3 peaks from 16 to 18 nm with the increase in sputtering pressure. In addition, a substantial decrease is observed in the intensity ratio of the UV exciton peak to the green emission peak (I_{UV}/I_{ge}) for the samples deposited at higher sputtering pressures. The small FWHM of the exciton peak and the higher value of I_{UV}/I_{ge} indicate the high optical quality of the samples. This reveals that the excitonic UV emission increases with a decrease in the grain interface area. Thus, the lower working pressure of 1.1×10^{-3} mbar is found to be optimum for producing better optical quality CuCl thin films.

IV. DISCUSSION

Variations observed in the film properties with the target to substrate spacing and working pressure motivate us to

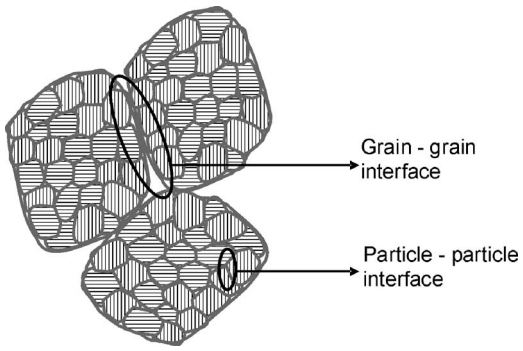

FIG. 6. Schematic representation of the "particle-particle" and "grain-grain" interfaces.

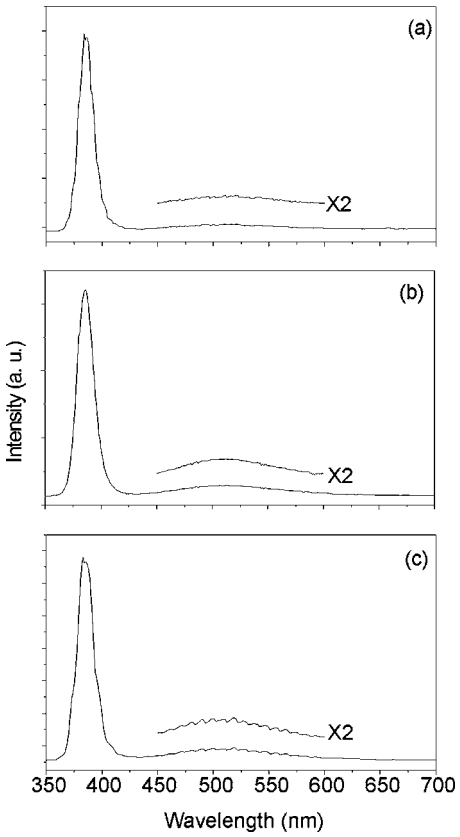

FIG. 7. CL spectra of CuCl films deposited at different sputtering pressures of (a) 1.1×10^{-3} mbar, (b) 6×10^{-3} mbar, and (c) 1×10^{-2} mbar.

investigate the underlying mechanisms. The kinetics of the formation of CuCl thin films is dependent on a number of factors including

(i) the intensity of fluxes of Cu and Cl arriving at the substrate,
(ii) the sticking coefficient/sticking probability of the particles reaching the substrate,
(iii) angular distribution of the fluxes arriving at the substrates,
(iv) desorption of the atoms on the surface, and
(v) mobility of the adatoms on the growing surface.

The compositional variation for different target to substrate positions observed from EDX analysis can be explained as follows. The mean free path of the particles was calculated to be around 3.3 cm at a working pressure of 2×10^{-3} mbar.[27] When the substrate is kept within a mean free path length, the sputtered neutrals reach the substrate with high energy (almost with their initial energy) with few collisions.[28] The higher energies make them more mobile, and it is more likely that free atoms will be desorbed. If the fluxes of Cu and Cl atoms from the target are equal, it is likely that any Cl atom on the surface will bond with the top layer as chlorine is highly electronegative (electronegativity of Cu and Cl is 1.90 and 3.16 Pauling units, respectively), whereas some Cu atoms may remain unbonded. These unbonded Cu atoms will more easily desorb from the substrate. This explains the presence of excess chlorine in the samples deposited with a target to substrate distance of ~3 cm.

As stated, when the substrate is positioned beyond the mean free path distance ($d_{ts}\geqslant4.5$ cm), the probability for collision of the sputtered particles increases, leading to a considerable energy loss.[28] When the particles lose their energy, they become less mobile on the substrate surface. The less mobile copper atoms may bond to the surface before they desorb and the desorption of Cu decreases with increase in the target to substrate spacing. This explains the significant increase of Cu content for $d_{ts}\geqslant4.5$ cm. The composition reaches the stoichiometry at $d_{ts}=6$ cm. For $d_{ts}>6$ cm, the films remain almost stoichiometric, as no considerable desorption of Cu atoms takes place.

The mobility of the sputtered particles decreases with increase in d_{ts}, and lower mobility of the particles on the substrate can yield less crystalline films.[29] This is related to the increase in FWHM of the CuCl (111) peak with increase in d_{ts} (see Fig. 3). The poor crystalline quality of the sample with $d_{ts}=4.5$ cm may be attributed to the presence of defects caused by slight compositional deviation causing an increased number of Cl interstitials and/or Cu vacancies (refer to Fig. 1).

Microstructural evaluation reveals that the grain interface area increases on increasing the working pressure. From the cathodoluminescence analysis, it is evident that the grain interface has a significant influence on the optical properties. Hence it is interesting to analyze the origin of the interface. The microstructural properties are influenced by the growth mechanisms of the films on the substrate surface. The film growth depends on several factors including the energy of the adatoms, substrate temperature, properties of the substrate, and substrate-film interface structure and energy.[30–32] In principle, the growth of crystalline films can have (i) a higher nucleation rate and/or (ii) faster grain growth, depending on the growth environment.

When the energy of the incoming particles to the substrate is lower, the particles are just adsorbed on the substrate surface as they are less mobile. These particles do not actively contribute to the grain growth by surface diffusion after nucleation on the growing surface. This favors the formation of a large number of nuclei rather than the spread of the existing nuclei by coalescing with the neighboring ones.[32] On the other hand, when the energy of the particles is higher, the particles are mobile enough to diffuse across the substrate surface and be captured by an existing nucleus. This speeds up grain growth, and grain growth is more favorable in this case.

At lower working pressures (1.1×10^{-3} mbar), the arriving particles are more mobile as they undergo fewer collisions, favoring grain growth, resulting in films with larger grains [Fig. 5(a)]. In contrast to this, at higher working pressures (1×10^{-2} mbar), the sputtered particles reaching the substrate are less energetic as they undergo a greater number of collisions in the plasma.[28] Therefore, the nucleation density is higher during growth, and the grown films consist of a larger number of smaller grains as can be observed in Fig. 5(b).

Grain boundaries are rich in (i) structural disorder, (ii) impurity segregation, and (iii) nonstoichiometry. With decreasing grain size, the surface to volume ratio becomes

larger, and hence smaller grains will have more nonradiative relaxation centers from the surface states.[33,34] The increased nonradiative relaxation results in the noticeable decrease in the UV excitonic emission intensity. Thus, the optical quality of the samples increases with the increase in grain size.

V. CONCLUSIONS

CuCl thin films were grown by the rf magnetron sputtering technique. The influences of target to substrate spacing and sputtering pressure on film properties are investigated in detail. The chemical stoichiometry was mainly controlled by the spacing between the target and the substrate. Microstructural evaluation revealed that the grain interface area of the film increases on increasing the working pressure. UV emission properties of the films were found to be influenced by the existence of meso- and nanostructural interfaces within the thin film. A combination of optimum target to substrate distance (6 cm) and sputtering pressure (1.1×10^{-3} mbar) yielded good optical quality CuCl films with an intense and sharp UV emission at room temperature.

ACKNOWLEDGMENTS

This project is funded by the Irish Research Council for Science Engineering and Technology (IRCSET) Grant No. SC/02/7. The authors would like to thank Billy Roarty for his technical support.

[1]S. Nakamura, M. Senoh, S. Nagahama, N. Iwasa, T. Yamada, T. Matsushita, H. Kiyoku, and Y. Sugimoto, Jpn. J. Appl. Phys., Part 2 **35**, L74 (1996).
[2]S. Guha and N. A. Bojarczuk, Appl. Phys. Lett. **72**, 415 (1998).
[3]J. W. Yang, A. Lunev, G. Simin, A. Chitnis, M. Shatalov, M. A. Kahn, J. E. Van Nostrand, and R. Gaska, Appl. Phys. Lett. **76**, 273 (2000).
[4]A. Ohtani, K. S. Stevens, and R. Beresfor, Appl. Phys. Lett. **65**, 61 (1994).
[5]J. A. Freitas, O.-H. Nam, R. F. Davis, G. V. Saparin, and S. K. Obyden, Appl. Phys. Lett. **72**, 2990 (1998).
[6]X. Li, S. G. Bishop, and J. J. Coleman, Appl. Phys. Lett. **73**, 1179 (1998).
[7]JCPDS Card No. 06-344 (International Centre for Diffraction, New York, 1997).
[8]JCPDS Card No. 27-1402 (International Centre for Diffraction, New York, 1997).
[9]M. Nakayama, H. Ichida, and H. Nishimura, J. Phys.: Condens. Matter **11**, 7653 (1999).
[10]B. Monemar, Phys. Rev. B **10**, 676 (1974).
[11]Y. R. Ryu, T. S. Lee, and H. W. White, Appl. Phys. Lett. **83**, 87 (2003).
[12]W. Chen, M. Dumas, S. Ahsan, A. Kahn, C. B. Duke, and A. Patton, J. Vac. Sci. Technol. A **10**, 2071 (1992).
[13]A. Yanase and Y. Segawa, Surf. Sci. **357/358**, 885 (1996).
[14]A. Yanase and Y. Segawa, Appl. Surf. Sci. **130–132**, 566 (1998).
[15]E. Vanagas, D. Brinkmann, J. Kudrna, O. Crégut, P. Gilliot, R. Tomasiunas, and B. Hönerlage, J. Phys.: Condens. Matter **14**, 3627 (2002).
[16]R. S. Williams, D. K. Shuh, and Y. Segawa, J. Vac. Sci. Technol. A **6**, 1950 (1988).
[17]N. Nishida, K. Saiki, and A. Koma, Surf. Sci. **324**, 149 (1995).
[18]G. R. Olbright and N. Peyghamberian, Solid State Commun. **58**, 333 (1986).
[19]K.-K. Kim, J.-H. Song, H.-J. Jung, W.-K. Choi, S.-J. Park, J.-H. Song, and J.-Y. Lee, J. Vac. Sci. Technol. B **18**, 286 (2000).
[20]D. H. Fan, Z. Y. Ning, and M. F. Jiang, Appl. Surf. Sci. **245**, 414 (2005).
[21]M. Jung, J. Lee, S. Park, H. Kim, and J. Chang, J. Cryst. Growth **283**, 384 (2005).
[22]H. C. Ong, J. Y. Dai, K. C. Hung, Y. C. Chan, R. P. H. Chang, and S. T. Ho, Appl. Phys. Lett. **77**, 1484 (2000).
[23]B. D. Cullity, *Elements of X-Ray Diffraction*, 2nd ed. (Addisson Wesley, Reading, MA, 1978).
[24]B. Lin, Z. Fu, and Y. Jia, Appl. Phys. Lett. **79**, 943 (2001).
[25]X. Liu, X. Wu, H. Cao, and R. P. H. Chang, J. Appl. Phys. **95**, 3141 (1998).
[26]T. Koida, S. F. Chichibu, A. Uedono, A. Tsukazaki, M. Kawasaki, T. Sota, Y. Segawa, and H. Koinuma, Appl. Phys. Lett. **82**, 532 (2003).
[27]B. Chapman, *Glow Discharge Processes* (Wiley, New York, 1980).
[28]J. A. Thornton, J. Vac. Sci. Technol. **11**, 666 (1974).
[29]J.-Y. Oh, J.-H. Lim, D.-K. Hwang, H.-S. Kim, R. Navamathavan, K.-K. Kim, and S.-J. Parkz, J. Electrochem. Soc. **151**, G623 (2004).
[30]A. Goswamy, *Thin Film Fundamentals*, 1st ed. (New Age International, New Delhi, 1996).
[31]D. M. Mattox, *Handbook of Physical Vapor Deposition (PVD) Processing* (Noyes, Park Ridge, NJ, 1998).
[32]A. Furuya, Y. Ohshita, and A. Ogura, J. Vac. Sci. Technol. A **18**, 2854 (2000).
[33]T. Matsumoto, H. Kato, K. Miyamoto, M. Sanoand, and E. A. Zhukov, Appl. Phys. Lett. **81**, 1231 (2002).
[34]K.-K. Kim, J.-H. Song, H.-J. Jung, W.-K. Choi, S.-J. Park, and J.-H. Song, J. Appl. Phys. **87**, 3573 (2000).